ρ-ω mixing and spin dependent charge-symmetry violating potential

Subhrajyoti Biswas,* Pradip Roy, and Abhee K. Dutt-Mazumder

Saha Institute of Nuclear Physics, 1/AF Bidhannagar, Kolkata-700 064, India

(Received 22 May 2008; revised manuscript received 2 September 2008; published 24 October 2008)

We construct the charge symmetry violating (CSV) nucleon-nucleon potential induced by the ρ^0-ω mixing due to the neutron-proton mass difference driven by the NN loop. Analytical expression for the two-body CSV potential is presented containing both the central and noncentral NN interaction. We show that the ρNN tensor interaction can significantly enhance the charge symmetry violating NN interaction even if the momentum dependent off-shell ρ^0-ω mixing amplitude is considered. It is also shown that the inclusion of form factors removes the divergence arising out of the contact interaction. Consequently, we see that the precise size of the computed scattering length difference depends on how the short-range aspects of the CSV potential are treated.

DOI: 10.1103/PhysRevC.78.045207 PACS number(s): 21.30.Fe, 13.75.Cs, 13.75.Gx, 21.65.Cd

I. INTRODUCTION

Charge symmetry violation (CSV), in itself, is an interesting physical phenomenon. While charge symmetry (CS) implies that the interaction between two neutrons or two protons is equal, but, in nature, this is found to be only approximately true. The violation of CS automatically violates charge independence (CI), however, the converse might not be always true [1–3]. It is possible to have CS even if the CI is violated which actually is a higher symmetry. The CSV, at the QCD level, is caused by the splitting of u-d quark masses.

Experimentally CSV can be observed at various levels. For instance, in NN interaction, the effect of CSV is traditionally inferred from the difference of the pp and nn scattering lengths in the ${}^1S_0$ state. The most recent scattering data [4–6] observe that the amount of CSV in the ${}^1S_0$ state is $\Delta a_{\rm CSV} = a^N_{pp} - a^N_{nn} = 1.6 \pm 0.6$ fm, where the superscript N indicates the 'nuclear' effect obtained after the electromagnetic (EM) corrections. Other convincing evidence of CSV NN interaction comes from the binding energy difference of mirror nuclei which is known as Okamoto-Nolen-Schifer (ONS) anomaly [7–9]. The modern manifestation of CSV includes difference of neutron-proton form factors, hadronic correction to $g-2$ [10] and the observation of the decay of $\Psi'(3686) \to (J/\Psi)\pi^0$, etc. [10].

In the present work we focus on the hadronic sector, and, in particular, we attempt to construct a CSV potential for the NN interaction in one boson exchange (OBE) model by invoking momentum dependent ρ^0-ω mixing. The fact that the neutron and proton masses are not degenerate means the various isospin pure resonant states like ρ^0-ω or π^0-η can, in reality, mix without violating any conservation principles dictated by other symmetries. In particular, the ρ^0-ω mixing seems to be a viable mechanism for the generation of significant amount of CSV [11–14]. The earlier construction of CSV potential involved on-shell mixing of the ρ^0 and ω meson states [14]. A whole class of phenomena including the difference of nn-pp scattering length, binding energy difference of ^{3}He-^{3}H, or ONS anomaly in general could be successfully explained via ρ^0-ω mixing [15].

However, in Ref. [16] such a success was severely criticized on grounds that the on-shell mixing amplitude differs quite significantly as one extrapolates the results from the ρ (or ω) pole to the space-like region which is relevant for the construction of the CSV potential. Goldman, Henderson, and Thomas [17] showed the strong $\mathbf{q}^2$ dependence of ρ^0-ω mixing to the CSV potential using a simple quark model. Similar results were reported in Refs. [16,18,19]. In Refs. [16–21] it was shown that such momentum dependencies suppress the contribution of ρ^0-ω mixing and also changes the sign of the mixing amplitude as one moves away from the ρ and ω poles.

On the other hand Miller [10] and Coon *et al.* [20] have advanced counter arguments that would restore the traditional role of ρ^0-ω mixing. The issue is still unresolved. Informative summaries of the controversial point of views can be found in Refs. [22–24]. Subsequently, several other calculations were also performed including the QCD sum rule [21,25] with varied conclusions.

Recently Machleidt and Müther [26] discussed various CSV mechanism to estimate the ${}^1S_0$ scattering length. Therefore, the issues, including ρ^0-ω mixing as the origin of the CSV force, seem to be quite open which provide part of the motivation of the present work.

Here we revisit the problem of ρ^0-ω mixing and invoke the mechanism adopted in [16], i.e., the mixing is driven by the neutron-proton mass difference. Although the driving mechanism is same, the main difference of our work with that presented in Ref. [16] resides in the treatment of the external legs. This is another source of CSV due to the nondegenerate nucleon mass. This, as we shall see, has serious consequences which even modify the central part of the CSV potential. We highlight the importance of the ρNN tensor interaction and show how this can counterbalance the weakening of the strength of the CSV interaction even when one extrapolates [11–13] the results from on-shell to off-shell.

The paper is organized as follows. In Sec. II we present the formalism where the three-momentum dependent ρ^0-ω mixing

*subhrajyoti.biswas@saha.ac.in

 ©2008 The American Physical Society

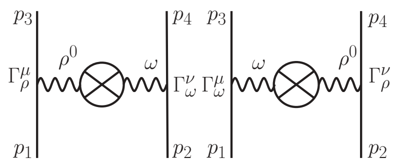

FIG. 1. Feynman diagrams for the mixing of isovector (ρ^0)-isoscalar (ω) mesons that contributes to the CSV NN interaction.

amplitude is used for the construction of CSV potential. The numerical results including the contributions of external legs and the ρNN tensor coupling to CSV potential are discussed in Sec. III. Finally, we summarize in Sec. IV.

II. FORMALISM

To calculate the ρ^0-ω mixing amplitude we use the following vector meson-nucleon interactions:

$$\mathcal{L}_{\omega NN} = g_\omega \bar{\Psi}\gamma_\mu \Phi^\mu_\omega \Psi, \tag{1a}$$

$$\mathcal{L}_{\rho NN} = g_\rho \bar{\Psi}\left[\gamma_\mu + \frac{C_\rho}{2M}\sigma_{\mu\nu}\partial^\mu\right]\tau\cdot\mathbf{\Phi}^\nu_\rho\Psi, \tag{1b}$$

where $C_\rho = f_\rho/g_\rho$ is the ratio of vector to tensor couplings. Ψ and Φ denote nucleon and meson fields, respectively. The tensor coupling of ω is not included in the present calculation because it is negligible in comparison to the vector coupling. All the parameters used in the present calculation are taken from those given by the Bonn group [27].

We now proceed to calculate the CSV potential using the Lagrangian described above. The corresponding Feynman diagrams are shown in Fig. 1. Here the CSV is represented by the crossed circles ($\Pi_{\rho\omega}(q^2)$). These parts, the external legs, depending upon whether we have a proton or neutron, serve as another source of CSV as mentioned in the Introduction due to their nondegenerate mass. Following Fig. 1 we write the matrix element as follows:

$$\mathcal{M}^{NN}_{\rho\omega}(q) = \left[\bar{u}_N(p_3)\Gamma^\mu_\rho u_N(p_1)\right]\Delta^\rho_{\mu\alpha}(q) \times \Pi^{\alpha\beta}_{\rho\omega}(q^2)\,\Delta^\omega_{\beta\nu}(q)\left[\bar{u}_N(p_4)\tilde{\Gamma}^\nu_\omega u_N(p_2)\right]. \tag{2}$$

The momentum space NN potential ($V^{NN}_{\rho\omega}(\mathbf{q})$) can be obtained by taking the limit $q_0 \to 0$ of $\mathcal{M}^{NN}_{\rho\omega}(q)$. Here $\Gamma^\mu_\omega = g_\omega\gamma^\mu$, $\tilde{\Gamma}^\nu_\rho = g_\rho[\gamma^\nu + \frac{C_\rho}{2M} i\sigma^{\nu\lambda}q_\lambda]$ denote the vertex factors and $\Pi^{\mu\nu}_{\rho\omega}(q^2)$ is the mixing amplitude (i.e., self-energy) driven by the difference between proton and neutron loops (see Fig. 2):

$$\Pi^{\mu\nu}_{\rho\omega}(q^2) = \Pi^{\mu\nu(p)}_{\rho\omega}(q^2) - \Pi^{\mu\nu(n)}_{\rho\omega}(q^2). \tag{3}$$

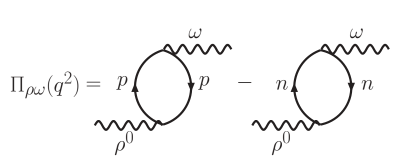

FIG. 2. The mixing amplitude driven by the difference between proton and neutron loops due to n-p mass difference.

The origin of the relative sign in the above equation is due to the different signs involved in the coupling of ω and ρ^0 with p and n [see Eqs. (1a)–(1b)]. It is to be noted that the ρNN vertex factor will have a relative sign depending upon whether it couples to p or n.This sign flip has been included.

The polarization tensor of ρ^0-ω mixing due to $N\bar{N}$ excitations is calculated using standard Feynman rules:

$$i\Pi^{\mu\nu(N)}_{\rho\omega}(q^2) = \int \frac{d^4k}{(2\pi)^4}\,\mathrm{Tr}\left[\Gamma^\mu_\omega G_N(k)\tilde{\Gamma}^\nu_\rho G_N(k+q)\right]. \tag{4}$$

Here $G_N(k)$ is the usual Feynman propagator given by

$$G_N(k) = \frac{\not{k} + M_N}{k^2 - M_N^2 + i\epsilon}. \tag{5}$$

After performing the trace of Eq. (4), one may write the polarization tensor as

$$\Pi^{\mu\nu(N)}_{\rho\omega}(q^2) = Q^{\mu\nu}\left[\Pi^{vv(N)}_{\rho\omega}(q^2) + \Pi^{tv(N)}_{\rho\omega}(q^2)\right], \tag{6}$$

where $Q^{\mu\nu} = (-g^{\mu\nu} + q^\mu q^\nu/q^2)$. The current conservation yields $q_\mu\Pi^{\mu\nu}_{\rho\omega}(q^2) = q_\nu\Pi^{\mu\nu}_{\rho\omega}(q^2) = 0$ as $q_\mu Q^{\mu\nu} = q_\nu Q^{\mu\nu} = 0$. From dimensional counting, it is clear that the integral in Eq. (4) is ultraviolet divergent. We use dimensional regularization [28–30] to isolate the divergent parts of the integral in Eq. (4) obtaining

$$\Pi^{vv(N)}_{\rho\omega}(q^2) = -\frac{g_\rho g_\omega}{2\pi^2}\left[\frac{1}{6\epsilon} - \frac{\gamma}{6} - \int_0^1 dx(1-x)x\ln \times\left(\frac{M_N^2 - x(1-x)q^2}{\Lambda^2}\right)\right]q^2, \tag{7a}$$

$$\Pi^{tv(N)}_{\rho\omega}(q^2) = -\frac{g_\rho g_\omega C_\rho}{8\pi^2}\left[\frac{1}{\epsilon} - \gamma - \int_0^1 dx\ln \times\left(\frac{M_N^2 - x(1-x)q^2}{\Lambda^2}\right)\right]q^2, \tag{7b}$$

where Λ is an arbitrary renormalization constant; γ is the Euler-Mascheroni constant. $\epsilon = 2 - D/2$ contains the singularity; $\epsilon \to 0$ as $D \to 4$. Since the mixing amplitude is the difference between proton and neutron loops contribution the divergent parts of the above expressions cancel out yielding,

$$\Pi^{vv}_{\rho\omega}(q^2) = \Pi^{vv(p)}_{\rho\omega}(q^2) - \Pi^{vv(n)}_{\rho\omega}(q^2) = \frac{g_\rho g_\omega}{2\pi^2}\int_0^1 dx(1-x)x\ln \times\left(\frac{M_p^2 - x(1-x)q^2}{M_n^2 - x(1-x)q^2}\right)q^2, \tag{8a}$$

$$\Pi^{tv}_{\rho\omega}(q^2) = \Pi^{tv(p)}_{\rho\omega}(q^2) - \Pi^{tv(n)}_{\rho\omega}(q^2) = \frac{g_\rho g_\omega C_\rho}{8\pi^2}\int_0^1 dx\ln\left(\frac{M_p^2 - x(1-x)q^2}{M_n^2 - x(1-x)q^2}\right)q^2, \tag{8b}$$

The full mixing amplitude thus becomes,

$$\Pi\rho\omega(q^2) = \Pi^{vv}_{\rho\omega}(q^2) + \Pi^{tv}_{\rho\omega}(q^2) = \frac{g_\rho g_\omega}{2\pi^2} q^2 \int_0^1 \left((1-x)x + \frac{C_\rho}{4}\right) \ln \times \left(\frac{M_p^2 - x(1-x)q^2}{M_n^2 - x(1-x)q^2}\right) dx. \quad (9)$$

Equation (9) displays the four-momentum dependence of the ρ^0-ω mixing amplitude in terms of three parameters g_ρ, g_ω, and C_ρ. We obtain $\Pi_{\rho\omega}(m_\omega^2) = -4314$ MeV^2 and $\Pi_{\rho\omega}(m_\rho^2) = -4152$ MeV^2. These are within the limit of experimentally extracted values ($\sim -4520 \pm 600$ MeV^2) [15]. Up to now our results are same as those of Ref. [16]. Note that most of the earlier efforts to understand the role of ρ^0-ω mixing in the CSV potential were based on the assumption of constant on-shell value for the mixing amplitude [12,15,26].

To calculate the CSV potential we have to use the mixing amplitude in the spacelike region ($q_0 \to 0$). As a result the mixing amplitude becomes $\mathbf{q}$ dependent, i.e., $\Pi_{\rho\omega}(0, \mathbf{q}) = \Pi_{\rho\omega}(\mathbf{q})$, where we find

$$\Pi_{\rho\omega}(\mathbf{q}) \simeq -\frac{g_\rho g_\omega}{12\pi^2}(2 + 3C_\rho)\ln(M_p/M_n)\mathbf{q}^2 \equiv -\mathcal{A}\mathbf{q}^2. \quad (10)$$

To calculate the CSV potential we take the nonrelativistic (NR) limits of Eq. (2). The relativistic energy E_N is expanded in powers of $\mathbf{q}^2$ and $\mathbf{P}^2$ keeping the lowest order in $\mathbf{q}^2/M_N^2(\mathbf{P}^2/M_N^2)$, i.e., $E_N \simeq M_N + \mathbf{P}^2/2M_N + \mathbf{q}^2/8M_N$. Here, $\mathbf{P} = \frac{1}{2}(\mathbf{p}_2 + \mathbf{p}_4) = -\frac{1}{2}(\mathbf{p}_1 + \mathbf{p}_3)$ is the average three-momentum of the nucleon. The three-momentum transfer is denoted by $\mathbf{q} = (\mathbf{p}_1 - \mathbf{p}_3) = (\mathbf{p}_4 - \mathbf{p}_2)$ (see Fig. 1). Also taking the NR limit of Dirac spinor and keeping terms $\mathcal{O}(\mathbf{P}^2/M_N^2)$ and $\mathcal{O}(\mathbf{q}^2/M_N^2)$ we obtain

$$u_N(\mathbf{p}_1) \simeq \left(1 - \frac{\mathbf{P}^2}{8M_N^2} - \frac{\mathbf{q}^2}{32M_N^2}\right)\begin{pmatrix} 1 \\ \frac{\sigma_1\cdot(\mathbf{P}+\mathbf{q}/2)}{2M_N}\end{pmatrix}, \quad (11)$$

where $\sigma_{1(2)}$ is the nucleon spin. The relevant expressions which will be needed to construct the momentum space potential are the following:

$$\bar{u}_N(\mathbf{p}_3)\gamma^0 u_N(\mathbf{p}_1) \simeq 1 + \left[\frac{\mathbf{P}^2}{4M_N^2} - \frac{\mathbf{q}^2}{16M_N^2} + i\frac{\sigma_1\cdot(\mathbf{q}\times\mathbf{P})}{4M_N^2}\right], \quad (12a)$$

$$\bar{u}_N(\mathbf{p}_3)\vec{\gamma} u_N(\mathbf{p}_1) \simeq \left[\sigma_1\left(\frac{\sigma_1\cdot\mathbf{p}_1}{2M_N}\right) + \left(\frac{\sigma_1\cdot\mathbf{p}_3}{2M_N}\right)\sigma_1\right], \quad (12b)$$

$$\bar{u}_N(\mathbf{p}_4)\sigma_{l0}q^l u_N(\mathbf{p}_2) \simeq i\left(\frac{\mathbf{q}^2}{2M_N^2}\right), \quad (12c)$$

$$\bar{u}_N(\mathbf{p}_4)\sigma_{lk}q^l u_N(\mathbf{p}_2) \simeq -(\sigma_2\times\mathbf{q})_k, \quad (12d)$$

where $(l, k) = 1, 2, 3$. A straight forward calculation using Eqs. (12a)–(12d) and Eq. (2) together with the NR meson propagators leads to the momentum space CSV potential due to ρ^0-ω mixing:

$$\begin{aligned} V^{NN}_{\rho\omega}(\mathbf{q}) = &-\frac{g_\rho g_\omega \Pi_{\rho\omega}(\mathbf{q})}{(\mathbf{q}^2+m_\rho^2)(\mathbf{q}^2+m_\omega^2)} \\ &\times\Bigg[T_3^+\Bigg\{\Bigg(1 + \frac{3\mathbf{P}^2}{2M_N^2} - \frac{\mathbf{q}^2}{8M_N^2} - \frac{\mathbf{q}^2}{4M_N^2}(\sigma_1\cdot\sigma_2) \\ &+ \frac{3i}{2M_N^2}\mathbf{S}\cdot(\mathbf{q}\times\mathbf{P}) + \frac{1}{4M_N^2}(\sigma_1\cdot\mathbf{q})(\sigma_2\cdot\mathbf{q}) \\ &+ \frac{1}{M_N^2}(\hat{\mathbf{q}}\cdot\mathbf{P})^2\Bigg) - \frac{C_\rho}{2M}\Bigg(\frac{\mathbf{q}^2}{2M_N} + \frac{\mathbf{q}^2}{2M_N}(\sigma_1\cdot\sigma_2) \\ &- \frac{2i}{M_N}\mathbf{S}\cdot(\mathbf{q}\times\mathbf{P}) - \frac{1}{2M_N}(\sigma_1\cdot\mathbf{q})(\sigma_2\cdot\mathbf{q})\Bigg)\Bigg\} \\ &- T_3^-\frac{C_\rho}{2M}\Bigg\{\Bigg(\frac{\mathbf{q}^2}{2M} - \frac{\mathbf{q}^2}{2M}(\sigma_1\cdot\sigma_2) \\ &+ \frac{1}{2M}(\sigma_1\cdot\mathbf{q})(\sigma_2\cdot\mathbf{q})\Bigg)\frac{\Delta M(1,2)}{M} \\ &- \frac{i}{M}(\sigma_1-\sigma_2)\cdot(\mathbf{q}\times\mathbf{P})\Bigg\}\Bigg]. \end{aligned} \quad (13)$$

Here $T_3^\pm = \tau_3(1) \pm \tau_3(2)$ and $\mathbf{S} = \frac{1}{2}(\sigma_1 + \sigma_2)$ is the total spin of the interacting nucleon pair. We define $M = (M_n + M_p)/2$, $\Delta M = (M_n - M_p)/2$, and $\Delta M(1, 2) = -\Delta M(2, 1) = \Delta M$. The spin dependent parts of the momentum space potential as found in Eq. (13) appear because of the contribution of the external legs shown in Fig. 1. On the other hand, $3\mathbf{P}^2/2M_N^2$ and $-\mathbf{q}^2/8M_N^2$ arise due to expansion of the relativistic energy E_N.

Note that the potential derived in Eq. (13) contains both class (III) and class (IV) potentials, and both of these potentials break the charge symmetry of NN interactions. The first part of this potential represents class (III) NN interaction which differentiates between nn and pp systems but vanishes for np system. On the other hand, the last part of Eq. (13) is a class (IV) NN interaction which exists for the np system only. In the present paper, we focus on the class (III) NN potential.

From Eq. (13) we extract a piece which, in coordinate space, gives rise to the δ-function potential. In momentum space it is given by

$$\delta V^{NN}_{\rho\omega} = g_\rho g_\omega \mathcal{A} T_3^+\left[\left(\frac{1+2C_\rho}{8M_N^2}\right) + \left(\frac{1+C_\rho}{4M_N^2}\right)(\sigma_1\cdot\sigma_2)\right]. \quad (14)$$

The problem of contact term can be avoided by using form factors, for which g_i is replaced with $g_i(\mathbf{q}^2)$:

$$g_i \to g_i(\mathbf{q}^2) = g_i\left(\frac{\Lambda_i^2 - m_i^2}{\Lambda_i^2 + \mathbf{q}^2}\right). \quad (15)$$

The cut-off parameters Λ_i govern the range of the suppression, which can be directly related to the hadron size. The values of Λ_is are determined from the fit of the two-nucleon empirical data [27,31].

The spin independent central part neglecting the contributions due to external legs and the ρNN tensor coupling, reduces to

$$V^0_{\rho\omega}(\mathbf{q}) = -\frac{g_\rho g_\omega \Pi_{\rho\omega}(\mathbf{q}) T_3^+}{(\mathbf{q}^2 + m_\rho^2)(\mathbf{q}^2 + m_\omega^2)}, \tag{16}$$

which is same as obtained in Ref. [16]. In coordinate space, treating the on-shell mixing amplitude to be constant one obtains

$$V^0_{\rho\omega}(\mathbf{r}) = -\frac{g_\rho g_\omega}{4\pi} \frac{\Pi_{\rho\omega}(m_\omega^2) T_3^+}{m_\omega^2 - m_\rho^2} \left[m_\rho Y_0(x_\rho) - m_\omega Y_0(x_\omega)\right], \tag{17}$$

where $Y_0(x_i) = e^{-x_i}/x_i$ and $x_i = m_i r$, $(i = \rho, \omega)$. With the form factors Eq. (17) reduces to

$$\begin{aligned} V^0_{\rho\omega}(\mathbf{r}) = &-\frac{g_\rho g_\omega}{4\pi} \frac{\Pi_{\rho\omega}(m_\omega^2) T_3^+}{m_\omega^2 - m_\rho^2} \left[\left\{\left(\frac{\Lambda_\omega^2 - m_\omega^2}{\Lambda_\omega^2 - m_\rho^2}\right) m_\rho Y_0(x_\rho)\right.\right. \\ &\left. - \left(\frac{\Lambda_\rho^2 - m_\rho^2}{\Lambda_\rho^2 - m_\omega^2}\right) m_\omega Y_0(x_\omega)\right\} \\ &+ \frac{m_\omega^2 - m_\rho^2}{\Lambda_\omega^2 - \Lambda_\rho^2}\left\{\left(\frac{\Lambda_\omega^2 - m_\omega^2}{\Lambda_\rho^2 - m_\omega^2}\right) \Lambda_\rho Y_0(X_\rho)\right. \\ &\left.\left. - \left(\frac{\Lambda_\rho^2 - m_\rho^2}{\Lambda_\omega^2 - m_\rho^2}\right) \Lambda_\omega Y_0(X_\omega)\right\}\right], \end{aligned} \tag{18}$$

where $X_i = \Lambda_i r$. Equation (18) represents the CSV potential with constant mixing amplitude neglecting the contribution of external legs. It is to be noted that in the limit $\Lambda_{\rho,\omega} \to \infty$, Equation (18) reduces to Eq. (17).

If we include the contribution of the external legs and ρNN tensor coupling, simplifies to the central part,

$$\begin{aligned} V^{0NN}_{\rho\omega}(\mathbf{r}) = &-\frac{g_\rho g_\omega}{4\pi} \mathcal{A} T_3^+ \left[\left(\frac{m_\rho^3 Y_0(x_\rho) - m_\omega^3 Y_0(x_\omega)}{m_\omega^2 - m_\rho^2}\right)\right. \\ &\left. + \frac{1 + 2C_\rho}{8M_N^2}\left(\frac{m_\rho^5 Y_0(x_\rho) - m_\omega^5 Y_0(x_\omega)}{m_\omega^2 - m_\rho^2}\right)\right]. \end{aligned} \tag{19}$$

In the above equation the first term in the bracket is same as one would have obtained from Eq. (16) by taking the momentum dependent mixing amplitude as in Eq. (10), while the second term contains the contribution coming from the Dirac spinors of the external lines. The latter, clearly involves ρNN vector and tensor interactions, and, as we shall see, the term containing the tensor coupling (C_ρ) is significantly larger compared to the vector interaction at distances below 0.75 fm or so.

We leave out the coordinate space contact terms from Eqs. (19) and (20). We also drop the term $3\mathbf{P}^2/2M_N^2$ from Eq. (13) while deriving the total coordinate space potential as it is not important in the present context. However, it should be noted that to fit the ${}^1S_0$ and ${}^3P_2$ phase shifts simultaneously this term is necessary as $\mathbf{P}^2$ gives the operator ∇_R^2 in coordinate space. Moreover, we use the $\mathbf{q}^2$ dependent mixing amplitude instead of constant on-shell value and for this we consider terms up to $\mathcal{O}(\mathbf{q}^2/M_N^2)$. Taking all this into consideration we obtain, after some algebraic manipulations, the coordinate space CSV potential as

$$\begin{aligned} V^{NN}_{\rho\omega}(\mathbf{r}) = &-\frac{g_\rho g_\omega}{4\pi} \mathcal{A} T_3^+ \left[\left(\frac{m_\rho^3 Y_0(x_\rho) - m_\omega^3 Y_0(x_\omega)}{m_\omega^2 - m_\rho^2}\right)\right. \\ &+ \frac{1}{M_N^2}\left(\frac{m_\rho^5 V_{vv}(x_\rho) - m_\omega^5 V_{vv}(x_\omega)}{m_\omega^2 - m_\rho^2}\right) \\ &\left. + \frac{C_\rho}{2M_N^2}\left(\frac{m_\rho^5 V_{tv}(x_\rho) - m_\omega^5 V_{tv}(x_\omega)}{m_\rho^2 - m_\omega^2}\right)\right]. \end{aligned} \tag{20}$$

The spin-spin, tensor, and spin-orbit interaction terms are explicitly contained in $V_{vv}(x)$ and $V_{tv}(x)$ which are as follows:

$$\begin{aligned} V_{vv}(x) = &\tfrac{1}{8} Y_0(x) + \tfrac{1}{6} Y_0(x)(\sigma_1 \cdot \sigma_2) \\ &- \tfrac{1}{12} Y_1(x) S_{12}(\hat{\mathbf{r}}) - \tfrac{3}{2} Y_2(x) \mathbf{L} \cdot \mathbf{S}, \end{aligned} \tag{21a}$$

$$\begin{aligned} V_{tv}(x) = &\tfrac{1}{2} Y_0(x) + \tfrac{1}{3} Y_0(x)(\sigma_1 \cdot \sigma_2) \\ &- \tfrac{1}{6} Y_1(x) S_{12}(\hat{\mathbf{r}}) - 2 Y_2(x) \mathbf{L} \cdot \mathbf{S}, \end{aligned} \tag{21b}$$

where

$$Y_1(x) = \left(1 + \frac{3}{x} + \frac{3}{x^2}\right) Y_0(x), \tag{22a}$$

$$Y_2(x) = \left(\frac{1}{x} + \frac{1}{x^2}\right) Y_0(x), \tag{22b}$$

$$S_{12}(\hat{\mathbf{r}}) = 3(\sigma_1 \cdot \hat{\mathbf{r}})(\sigma_2 \cdot \hat{\mathbf{r}}) - (\sigma_1 \cdot \sigma_2). \tag{22c}$$

The first part of Eq. (20) represents the central part without contributions from external legs. In addition, the last two terms of Eq. (20) are the contributions coming from the external nucleon legs as discussed earlier. It is also to be noted that the central part also receives contributions due to the presence of the first terms in Eqs. (21a) and (21b). The tensor contribution (C_ρ) of ρ-meson is contained in the third term of Eq. (20).

Equation (20) does not include form factors. It diverges near the core. This divergence can be removed by incorporating form factors as in Eq. (15). Thus the complete CSV potential with form factors reduces to

$$\begin{aligned} V^{NN}_{\rho\omega}(\mathbf{r}) = &-\frac{g_\rho g_\omega}{4\pi} \frac{\mathcal{A} T_3^+}{m_\omega^2 - m_\rho^2} \left[\left\{\left(\left(\frac{\Lambda_\omega^2 - m_\omega^2}{\Lambda_\omega^2 - m_\rho^2}\right) m_\rho^3 Y_0(x_\rho)\right.\right.\right. \\ &\left. - \left(\frac{\Lambda_\rho^2 - m_\rho^2}{\Lambda_\rho^2 - m_\omega^2}\right) m_\omega^3 Y_0(x_\omega)\right) \\ &+ \frac{1}{M_N^2}\left(\left(\frac{\Lambda_\omega^2 - m_\omega^2}{\Lambda_\omega^2 - m_\rho^2}\right) m_\rho^5 V_{vv}(x_\rho)\right. \\ &\left. - \left(\frac{\Lambda_\rho^2 - m_\rho^2}{\Lambda_\rho^2 - m_\omega^2}\right) m_\omega^5 V_{vv}(x_\omega)\right) \\ &+ \frac{C_\rho}{M_N^2}\left(\left(\frac{\Lambda_\omega^2 - m_\omega^2}{\Lambda_\omega^2 - m_\rho^2}\right) m_\rho^5 V_{tv}(x_\rho)\right. \\ &\left.\left. - \left(\frac{\Lambda_\rho^2 - m_\rho^2}{\Lambda_\rho^2 - m_\omega^2}\right) m_\omega^5 V_{tv}(x_\omega)\right)\right\} \end{aligned}$$

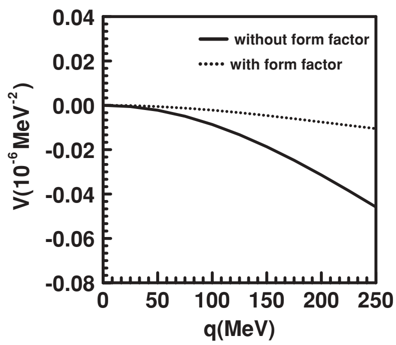

FIG. 3. The ρ^0-ω mixing contribution to the central part of the CSV NN potential in momentum space [Eq. (16)] is presented here. The dotted and solid curves present the three-momentum dependent potential with and without form factor, respectively.

$$
\begin{aligned}
&+\left(\frac{m_\omega^2-m_\rho^2}{\Lambda_\omega^2-\Lambda_\rho^2}\right)\Bigg\{\Bigg(\left(\left(\frac{\Lambda_\omega^2-m_\omega^2}{\Lambda_\rho^2-m_\omega^2}\right)\Lambda_\rho^3 Y_0(X_\rho)\right.\\
&-\left.\left(\frac{\Lambda_\rho^2-m_\rho^2}{\Lambda_\omega^2-m_\rho^2}\right)\Lambda_\omega^3 Y_0(X_\omega)\right)\\
&+\frac{1}{M_N^2}\left(\left(\frac{\Lambda_\omega^2-m_\omega^2}{\Lambda_\rho^2-m_\omega^2}\right)\Lambda_\rho^5 V_{vv}(X_\rho)\right.\\
&-\left.\left(\frac{\Lambda_\rho^2-m_\rho^2}{\Lambda_\omega^2-m_\rho^2}\right)\Lambda_\omega^5 V_{vv}(X_\omega)\right)\\
&+\frac{C_\rho}{2M_N^2}\left(\left(\frac{\Lambda_\omega^2-m_\omega^2}{\Lambda_\rho^2-m_\omega^2}\right)\Lambda_\rho^5 V_{tv}(X_\rho)\right.\\
&-\left.\left(\frac{\Lambda_\rho^2-m_\rho^2}{\Lambda_\omega^2-m_\rho^2}\right)\Lambda_\omega^5 V_{tv}(X_\omega)\right)\Bigg\}\Bigg].
\end{aligned}
\tag{23}
$$

Note that the above equation contains the contribution of Eq. (14). The CSV NN potential given in Eq. (23) can be used to calculate the difference between nn and pp scattering lengths at ${}^1S_0$ state. The difference between scattering lengths, $\Delta a = a_{pp} - a_{nn}$, and the difference between the CSV nn and

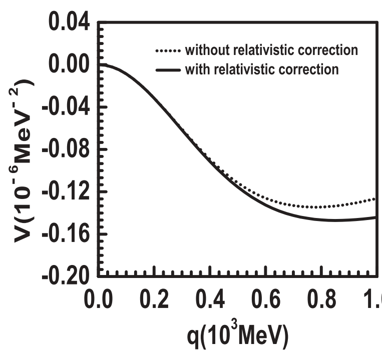

FIG. 4. Central part of momentum space potential without (dotted curve) and with (solid curve) the relativistic correction.

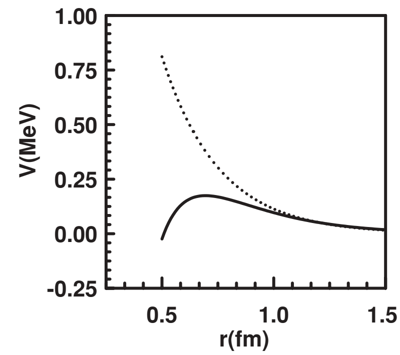

FIG. 5. Central part of the coordinate space potential without form factors. The potentials considering the constant on-shell mixing amplitude (dotted curve) and three-momentum dependent mixing amplitude (solid curve) without external legs and ρNN tensor contributions.

pp potentials, $\Delta V_{\rho\omega} = V_{\rho\omega}^{nn} - V_{\rho\omega}^{pp}$, are related by

$$
\Delta a = -a^2 M \int_0^\infty \Delta V_{\rho\omega}\, u_0^2(r)\, dr, \tag{24}
$$

where $a^2 = a_{nn}a_{pp}$ and $u_0(r)$ is the zero energy wave function, normalized to approach $1 - r/a$ as $r \to \infty$ and $u(0) = 0$. To calculate Δa we use the following zero energy wave function [32]:

$$
u_0(r) = \left[1 - \frac{r}{a}\right] - \left[\gamma(1-\lambda)\frac{r}{2} + (1+\lambda)\right]\frac{e^{-\gamma r}}{1+\lambda e^{-\gamma r}}, \tag{25}
$$

where $\lambda = (1 - 2r_0/a)^{-1/2}$, $\gamma = 2(1+\lambda)/(r_0\lambda)$ and r_0 is the effective range. In the present calculation we take $r_0 = 2.8$ fm.

III. RESULTS

In this section we present our results. First we show the momentum space central potential [see Eq. (16)] in Fig. 3 considering the three-momentum dependent mixing

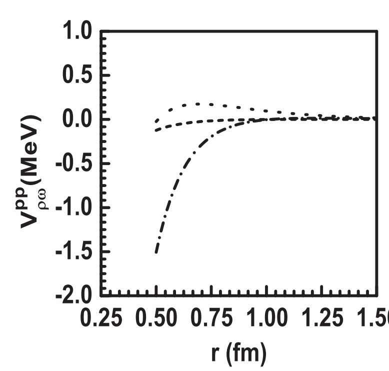

FIG. 6. The dotted curve represents only the central part [Eq. (19)]. The external legs and the ρNN tensor contributions to the central potential are shown by dashed and dot-dashed curves, respectively.

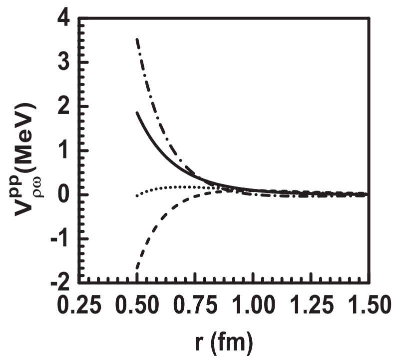

FIG. 7. The coordinate space $V^{pp}_{\rho\omega}$ potential without form factors, at the $^1S_0$ state. Different parts of the CSV potential, i.e., the central (dotted), central with external legs plus the ρNN tensor contribution (dashed), and the spin dependent (dashed-dotted) parts are presented here. The solid curve shows the total CSV potential.

amplitude. In this figure the dotted curve represents the central potential with the form factor in the spacelike region. In contrast, the solid curve represents the same without the form factor [1,33].

In Fig. 4 the importance of the relativistic correction to the central part potential in momentum space is displayed. This correction, as expected, is marginal at low momentum (below $|\mathbf{q}| \sim 500$ MeV) transfer. In the short distance regime, i.e., near the core region, the relativistic correction becomes significant which is clearly seen in Fig. 4.

In Fig. 5 we show the central part of the potential due to both on-shell and off-shell mixing amplitudes. It is seen that the contribution of the off-shell ρ^0-ω mixing amplitude to the NN potential is opposite in sign relative to the contribution obtained from using the on-shell value. This, again, is consistent with the observation made in Ref. [16].

The individual contribution of different parts of the central potential given in Eq. (19) is presented in Fig. 6. Clearly the contribution of ρNN tensor coupling to the CSV potential is found to be much larger than the contribution of the first part (i.e., the central part without external legs and ρNN tensor

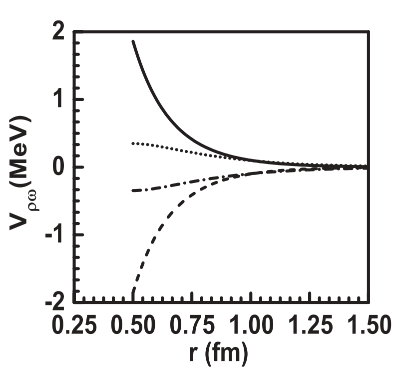

FIG. 8. Total $^1S_0$ CSV potential without form factors for the pp and nn systems are denoted by the solid and the dashed curves, respectively. The same are presented by dotted and dashed-dotted curves without ρNN tensor contribution.

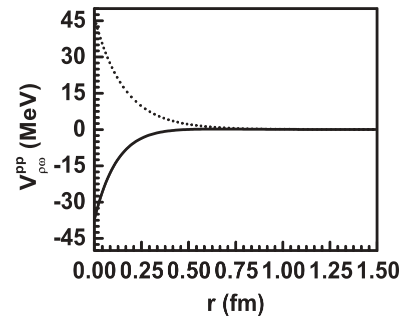

FIG. 9. Total $^1S_0$ CSV potential with form factors [Eq. (23)] for the pp system is presented by the solid curve and dotted curve shows the same without $\delta V^{pp}_{\rho\omega}$.

contribution). It is to be noted that the ρNN tensor contribution is present only when the external legs are taken into account.

The $^1S_0$ state CSV potential for the pp system due to ρ^0-ω mixing is shown in Fig. 7. The importance of the central part with relativistic correction (dashed curve) and tensor contribution (dashed-dotted curve) are clearly revealed. The magnitude of the contribution of tensor coupling is comparable with that of the central part with relativistic correction in the core region. On the other hand, magnitude of the contribution of tensor coupling is found to be much larger than the contribution of the central part (dotted curve) without relativistic correction in the core region. In the dynamical region, it is seen that all the contributions are comparable. The solid curve in this figure represents the total contribution together with the relativistic correction.

In Fig. 8 we present the CSV potential at the $^1S_0$ state both for the pp and nn systems. The solid and dashed curves, respectively, show the CSV potential for the pp and nn systems taking the contribution of the tensor coupling of the ρ-meson. The same are presented by dotted and dot-dashed curves without considering the tensor coupling.

The $^1S_0$ CSV potential with form factors is displayed in Fig. 9. It is seen that the inclusion of $\delta V^{NN}_{\rho\omega}$ modifies the CSV potential dramatically. It is to be noted that, with its inclusion, the CSV potential changes its sign.

The difference in scattering length Δa when calculated with the potential of Eq. (23) is also markedly different from that calculated ignoring the term $\delta V^{NN}_{\rho\omega}$. The results of Δa with and without $\delta V^{NN}_{\rho\omega}$ are shown in Table I.

IV. SUMMARY AND DISCUSSION

In the present work we have constructed the CSV potential within the framework of the OBE model and studied the

TABLE I. The difference between pp and nn scattering lengths at $^1S_0$.

	$\Delta a(C_\rho = 0)$ (fm)	$\Delta a(C_\rho = 6.1)$ (fm)
Without $\delta V^{NN}_{\rho\omega}$	0.31	2.14
With $\delta V^{NN}_{\rho\omega}$	−0.06	−0.08

role of three-momentum dependence ρ^0-ω mixing amplitude in CSV. We find that the inclusion of the contributions coming from the external legs are important because of the strength of the ρNN tensor interactions. It is seen that unlike the previous finding [16] where the charge symmetry violation at the external legs were ignored, the strength of the CSV interaction could be significantly larger even when the off-shell amplitude for the ρ^0-ω mixing is considered. It is important to note that contribution from the spinors also modifies the central part of the two body potential as shown in Eqs. (19) and (20). Furthermore, we present results both for the central and noncentral part of the CSV potential.

We also have calculated difference of $^1S_0$ scattering lengths between *pp* and *nn* systems and explicitly show the contribution of $\delta V_{\rho\omega}^{NN}$. It is to be noted that Δa changes sign with the inclusion of the fourier transform of $\delta V_{\rho\omega}^{NN}$. It would be interesting to apply the potential presented here to calculate various other CSV observables to delineate the role of tensor interaction further.

[1] M. St. Stevens, Phys. Lett. **19**, 499 (1965).
[2] B. W. Downs and Y. Nogami, Nucl. Phys. **B2**, 459 (1967).
[3] E. M. Henley and T. E. Keliher, Nucl. Phys. **A189**, 632 (1972).
[4] G. A. Miller, M. K. Nefkens, and I. Slaus, Phys. Rep. **194**, 1 (1990).
[5] C. R. Howell *et al.*, Phys. Lett. **B444**, 252 (1998).
[6] D. E. Gonzalez Trotter *et al.*, Phys. Rev. Lett. **83**, 3788 (1999).
[7] J. A. Nolen and J. P. Schiffer, Annu. Rev. Nucl. Sci. **19**, 471 (1969).
[8] K. Okamoto, Phys. Lett. **11**, 150 (1964).
[9] L. N Epele, H. Fanchlottl, C. A. Garcia Canal, and G. A. Gonzfilez Sprlnberg, Phys. Lett. **B277**, 33 (1992).
[10] G. A. Miller, A. K. Opper, and E. J. Stephenson, nucl-ex/0602021.
[11] E. M. Henley and G. A. Miller, in *Mesons in Nuclei*, edited by M. Rho and D. H. Wilkinson (North-Holland, Amsterdam, 1979).
[12] Peter C. McNamee, Michael D. Scadron, and Sydney A. Coon, Nucl. Phys. **A249**, 483 (1975).
[13] S. A. Coon and M. D. Scadron, Nucl. Phys. **A287**, 381 (1977).
[14] P. G. Blunden and M. J. Iqbal, Phys. Lett. **B198**, 14 (1987).
[15] S. A. Coon and R. C. Barrett, Phys. Rev. C **36**, 2189 (1987).
[16] J. Piekarewicz and A. G. Williams, Phys. Rev. C **47**, R2462 (1993).
[17] T. Goldman, J. A. Henderson, and A. W. Thomas, Few-Body Syst. **12**, 123 (1992).
[18] G. Krein, A. W. Thomas, and A. G. Williams, Phys. Lett. **B317**, 293 (1993).
[19] H. B. O'Connell, B. C. Pearce, A. W. Thomas, and A. G. Williams, Phys. Lett. **B336**, 1 (1994).
[20] S. A. Coon, B. H. J. McKellar, and A. A. Rawlinson, in *Intersections Between Particle and Nuclear Physics*, edited by T. W. Donelly, AIP Conf. Proc. No. 412 (AIP, Woodbury, NY, 1997), p. 368.
[21] T. Hatsuda, E. M. Henley, Th. Meissner, and G. Krein, Phys. Rev. C **49**, 452 (1994).
[22] G. A. Miller and W. H. T. van Oers, in *Symmetries and Fundamental Interactions in Nuclei*, edited by W. C. Haxton and E. M. Henley (World Scientific, Singapore, 1995), p. 127.
[23] H. B. O'Connell, B. C. Pearce, A. W. Thomas, and A. G. Williams, Prog. Part. Nucl. Phys. **39**, 201 (1997).
[24] S. A. Coon and M. D. Scadron, Proceedings of the XXIII Symposium on Nuclear Physics, Oaxtepec, Mexico, 2000 (Revista Mexicana de Fisica, to be published).
[25] A. K. Dutt-Mazumder, R. Holfman, and M. Pospelov, Phys. Rev. C **63**, 015204 (2000).
[26] R. Machleidt and H. Müther, Phys. Rev. C **63**, 034005 (2001).
[27] R. Machleidt, K. Holinde, and Ch. Elster, Phys. Rep. **149**, 1 (1987).
[28] G. 't Hooft and M. T. Veltmann, Nucl. Phys. **B44**, 189 (1973).
[29] M. E. Peskin and D. V. Schroeder, *An Introduction to Quantum Field Theory* (Addison-Wesley Publishing Company, Reading, MA, 1995).
[30] T. P. Cheng and L. F. Li, *Gauge Theory of Elementary Particles* (Clarendon Press, Oxford/New York, 2006).
[31] R. Machleidt, *Proceedings of the Relativistic Dynamics and Quark-Nuclear Physics* (Wiley, New York, 1986).
[32] M. W. Kermode and W. van Dijk, Phys. Rev. C **42**, 1891 (1990).
[33] C. Yalcin, M. Halil, and E. Aksahin, Phys. Scr. **20**, 36 (1979).